Submitted to SPIE journal

An X-Ray Detector for Time-Resolved Studies

59

Brian Rodricks and Christine Brizard

Advanced Photon Source-Argonne National Laboratory
Argonne, IL 60439

Roy Clarke

Department of Physics-The University of Michigan
Ann Arbor, MI 48109-1120

Walter Lowe

AT&T Bell Laboratories
Murray Hill, NJ 07974

DRAFT

ABSTRACT

The development of ultrahigh-brightness x-ray sources makes time-resolved x-ray studies more and more feasible . Improvements in x-ray optics components are also critical for obtaining the appropriate beam for a particular type of experiment. Moreover, fast parallel detectors will be essential in order to exploit the combination of high intensity x-ray sources and novel optics for time-resolved experiments. A CCD detector with a time resolution of microseconds has been developed at the Advanced Photon Source (APS). This detector is fully programmable using CAMAC electronics and a MicroVax computer. The techniques of time-resolved x-ray studies, which include scattering, microradiography, microtomography, stroboscopy,etc., can be applied to a range of phenomena (including rapid thermal annealing, surface ordering, crystallization, and the kinetics of phase transition) in order to understand these time-dependent microscopic processes. Some of these applications will be illustrated by recent results performed at synchrotrons. New powerful x-ray sources now under construction offer the opportunity to apply innovative approaches in time-resolved work.

1. INTRODUCTION

The increasing availability of very high intensity x-ray beams generated by synchrotron storage rings makes possible new kinds of structural kinetics studies.[1] The facilities being developed will provide powerful probes into time-dependent effects such as fast phase transition kinetics, lattice relaxation, and other transient processes in materials. To date, time scales for x-ray measurements have generally been greater than 1 second limiting structural measurements to those changes that evolve slowly or can be frozen at the point of interest. A case in point is the temperature driven first-order phase transition that has been examined both above and below the transition temperature, but not through it. Another important example is the relaxation of strain in superlattices and thin films.[2] The two major impediments to time-resolved x-ray scattering (TRXRS) have been the lack of both

RODRICKS

high brightness x-ray sources and fast position sensitive detectors. Progress has been made in both of these areas with the advent of dedicated synchrotron radiation sources and semiconductor-based position detectors.[3] The future looks even more promising with the construction of third generation synchrotrons like the 7-GeV Advanced Photon Source (APS) at Argonne National Labratory, the 1.5-GeV Advanced Light Source (ALS) at Lawerence Berkeley Laboratory, and the 6-GeV European Synchrotron Radiation Facility (ESRF) in Grenoble.

2. CCD DETECTOR

This entirely new programmable CCD detector developed at the Advanced Photon Souce (APS) has already been described in detail elsewhere.[4] The general system architecture is shown in Fig. 1. The MicroVax III computer controls a CAMAC set of electronics that possesses modules for read-out waveforms, data digitization, buffer memory and display, all of which interact with a local LSI-11 microprocessor. The flexibility rsults from the interaction between the LSI-11, the MicroVax, and all other modules. The communication between the LSI-11 microprocessor and the electronic modules is done through flags called look-at-me (LAM) signals.The waveforms used in order to read-out the CCD chip are provided by programmable waveform generators. For a chip comprised of n rows and m columns, the read-out consists in m serial transfers after each parallel transfer and this sequence is repeated n times to read-out the whole chip. The waveform generator module memories contain the information of the number of columns and the microprocessor contains the information of the number of rows of the chip. Appropriate waveform trains with m periods are sent out from the waveform generator in order to read-out one row of the chip. The microprocessor allows this procedure to occur n times, after which it sends a message to the MicroVax computer to inquire what needs to be done next. The CCD output signal is preamplified by an on-chip amplifier (1 μV/e) and, after further amplification, digitized by a 12-bit ADC, and stored in a 12x1Mb buffer memory. The KineticSystems Corporation 2-channel transient recorder allows one to simultaneously digitize the data and other parameters that may be varied (like temperature or pressure) during a time-resolved experiment. The data can be directly viewed on a high resolution color video monitor (1024x1024 pixels) through a high resolution display driver. This feature is extremely convenient for on-line diagnostics during experiments. The data can also be transferred to the MicroVax III computer hard disk.

The Peltier cooled CCD chip (-40^{o}C) is physically placed on a customized PC board inside a small vacuum chamber to prevent condensation on its sensitive front surface. Two vacuum chamber front-ends are available. For visible imaging, the vacuum chamber is composed of a quartz window on which lenses can be adapted. For direct x-ray imaging, the vacuum chamber has a beryllium window.

The CCD used in the experiments described here is the Texas Instruments TI 4849 "virtual phase" chip,[5] consisting of 584 rows of pixels arranged in 390 columns. Each pixel is 22.4 μm^2 with a full-well capacity of $2x10^5$ electrons. The virtual phase technology requires only three waveforms. The parallel waveform transfers one row down the array while the serial waveform takes each row of data from the serial register and transfers it through an on-chip amplifier out of the device. Finally, the reset waveform resets the on-chip amplifier after every serial transfer. Fig. 2 defines the primary waveforms and transition timings, which are both programmable quantities.[6]

There are various modes of detector operation that are exploited at various stages of the experiment. There are three primary modes of read-out and the integration time is programmable for each. In the first mode, which is the full frame mode, the entire device is active and is read-out after a preprogrammed integration period. In the second mode, an x-ray mask is placed over the detector with a predefined number of rows being active. During an experiment, this row slice acts as a linear detector where a few rows are summed in the serial register and then read-out to the computer along with a time stamp. By summing over a number of rows, the statistics can be improved with minimum reduction in speed. This is because the parallel transfer time is much faster than the serial transfer. This mode gives a time resolution of 20ms. The third mode uses an x-ray mask with one active row near the top of the device. In this mode, the detector acts as a storage device where data is swept down the rows by temporarily disabling the serial waveform and sending the parallel waveform 584 times till the entire device is full and then, the entire frame is read to the computer. This mode gives us a time resolution of 25 μs, but limits us to a maximum of 584 rows. All time-resolved experiments were performed under direct x-ray illumination.

3. TIME-RESOLVED X-RAY EXPERIMENTS

3.1 Minute-scale experiment

Some x-ray time-resolved experiments need to be performed on a time scale on the order of a few minutes to have reasonably good statisitics. This is, for example, the case for diffraction from amorphous metallic alloys[7] or its early crystallized products. Metallic glasses, regardless of the way they are prepared, are not in configurational equilibrium but are relaxing slowly by a homogeneous process towards an "ideal" metastable amorphous state of lower energy. This system possesses the inherent possibility of transforming into a more stable crystalline state. Understanding the micromechanisms of crystallization in order to impede or control crystallization is therefore, a prerequisite for most applications. The crystallization of the Fe-B system has been studied by several methods: differential scanning calorimetry (DSC),[8] x-ray diffraction,[9] Mössbauer spectroscopy,[10] and scanning electron (SEM) and transmission electron (TEM) microscopy[11].

The CCD detector has been used to study the early stages of crystallization of $Fe_{80}B_{20}$ during *in situ* x-ray diffraction at the National Synchrotron Light Source (NSLS). The details and analysis of this experiment are the subject of another publication.[12] The double-crystal monochromator of the X6 beamline at NSLS was set at 7 KeV, below the fluorescence edge of Fe. The $Fe_{80}B_{20}$ samples are resistively heated in a vacuum chamber in order to prevent Fe oxidation. The two-dimensionality of the detector presents, in this case, two main advantages. First, full diffraction patterns within a large field of view (a few degrees) can be recorded on a one shot basis. Second, because of the geometry used to study these polycrystalline samples, the diffracted peaks can be adjusted to be parallel to the columns of the CCD chip, hence the rows can be summed. This technique allows one to increase the statistics by a factor up to 1000 for a typical 1024 row CCD chip. This *in situ* x-ray diffraction has shown the growth of three different phases (Fe_3B, α-Fe, Fe_2B) during the crystallization process. Diffracted peaks corresponding to these three different phases can be seen in Fig. 3. The peaks correspond to row sums. The main peak

corresponds to the cubic α–Fe (110) and the tetragonal Fe_3B (330), (112) reflections (2θ=51.8 deg.). The smaller peak corresponds to the Fe_3B (321) reflection (2θ=50.2 deg.). The amount of crystallized Fe_3B doesn't change at 400 deg. C, but decreases at 500 deg. C and disappears at 600 deg. C (metastable phase). The intensities of the (321) and (330), (112) Fe_3B peaks are comparable (Table I). At 300 deg. C, the main peak is much more intense than the (321) Fe_3B peak. Both phases α-Fe and Fe_3B appear in the same range of temperature around 300 deg. C (eutectic crystallization). Then, the part of the crystallized hypo-eutectoid alloy (α-Fe) keeps increasing from 300 deg. C to 600 deg. C. For temperatures higher than 500 deg. C, the main peak presents a shoulder at an angle 0.4^o higher than the peak maximum position. This additional peak is clearly visible for a more advanced crystallization and corresponds to the primitive tetragonal Fe_2B (211) peak. The appearance of this Fe_2B phase is clearly linked with the disappearance of the Fe_3B phase. The integrated intensity doesn't change much with temperature. On the other hand, the maximum intensity increases significantly with temperature. From 300 to 600 deg. C, the crystallized fraction doesn't increase much, but the grain size increases through conglomeration. α-Fe coalesces and precipitates out of the matrix. This is in good agreement with previous work.[13] The numerous small nuclei get transformed into larger nuclei.

The high dynamic range of the detector enables one to look at very different intense peaks, such as α-Fe and Fe_2B, at the same time. An interesting experiment would be to perform a similar *in situ* x-ray diffraction in order to study the crystallization of $Fe_{75}B_{25}$. At temperatures less than 900 deg. C, this system decomposes only into Fe_3B, so the kinetics should be faster.[14]

3.2 Millisecond-scale experiment

The energy dispersive beam characteristics, due to a tunable asymmetrically cut Ge(111) curved crystal monochromator coupled to the CCD position sensitive detector, enables one to obtain complete diffraction spectra with no moving parts.[15] This arrangement allows one to study transient behavior as it occurs. Rapid thermal annealing experiments were performed on strained molecular beam epitaxy (MBE) grown superlattices with a time resolution of 100 milliseconds.[16] The strain relaxation during rapid thermal annealing shows that the lattice of an as-grown quantum well structure is relieved cooperatively by a series of sluggish discontinuous transitions. Well-defined metastable states of strain are observed between the transitions.

3.3 Microsecond-scale experiment

As a final test of the detector, a diffraction experiment from Si(400) was performed primarily to test the maximum speed at which it could be driven. Starting with a few hundred microseconds, diffraction data were accumulated down to 25 microseconds. The large capacitance of the CCD restricted the minimum gap between parallel transfers to 20 microseconds. Oscillations of the beam due to the vibrations of the Ge(111) crystal when the photon shutter was opened are observed on such "x-ray movies" performed on a

microsecond time scale.[17] To do this fast experiment, we kept the photon shutter open and used the safety shutter upstream to control the beam.

4. CONCLUSION

A new programmable CCD detector has been developed for imaging,[18] time-resolved experiments and other synchrotron applications. The versatility of this CAMAC-based system allows one to use most commercially available CCD chips. Various CCD chips with different formats and read-out waveforms have been successfully used. Various time-resolved experiments have been performed using the three different modes of the CCD detector. This device can monitor rapid thermal annealings, strain relaxations, crystallization kinetics,etc.. by recording x-ray movies on time scales from minutes to a few microseconds. The innovative technique used here opens new exciting fields for the study of transient behaviors in matter.

5.ACKNOWLEDGEMENTS

It is a pleasure to thank Gopal Shenoy and Dennis Mills for their great support; also Joe Arko and Ron Hopf for their invaluable help assisting us in building this new detector. This work is supported by U.S. Dept. of Energy, BES-Materials Science, under grant contract #W-31-109-ENG-38. The authors wish to acknowledge also the support of the Army Research Office (URI Program) under contract DAAL-03-87-K0007 and NSF grant DMR 8805156.

6.REFERENCES

1. D.M. Mills, "Time-resolved studies" in Handbook on Synchrotron Radiation, Vol. 3, ed. D. Moncton and G. Brown (1991).

2. J.M. Gibson, L.R. Dawson, "Layered stuctures, epitaxy and interfaces, MRS Symposia Proceedings No. 37 (Materials Research Society, Pittsburgh, 1985).

3. J.G. Timothy , R.P. Madden, "Photon detectors for the ultraviolet and x-ray region" in Handbook on Synchrotron Radiation, Vol. 1a, ed. by E.E. Koch (1983).

4. C. Brizard, B. Rodricks, "Programmable CCD imaging system for synchrotron radiation studies," to be published in Rev. Sci. Instrum.

5. J. Janesick, IEEE Trans. Electron Dev. 28, 483 (1981).

6. B. Rodricks, C. Brizard, "Programmable CCD imaging detector for synchrotron radiation experiments," submitted to Nucl. Instrum. and Methods.

7. F.E. Luborsky, "Amorphous metallic alloys," butterwoths Monographs in Materials (1983).

8. E.E. Alp, K.M. Simon, M. Saporoschenko, W.E. Brower, Jr., J. Non-Crys. Sol. **61-62**, 871 (1984).

9. J.M. Dubois, G. Lecaer, Phys. Stat. Sol., **a64**, 275 (1981).

10. E.E. Alp, Thesis, Southern Illinois University (1984).

11. A.L. Greer, J. Non-Crys. Sol., **61-62**, 737 (1984).

12. C. Brizard, B. Rodricks, E. Alp, R. MacHarrie, "Early stages of the crystallization of $Fe_{80}B_{20}$," to be submitted to J. of Mater. Science.

13. O.T. Inal, L. Keller, J. Mater. Sci.**15** 1947-1961 (1980) .

14. M. Takahashi, M. Koshimura, T. Abuzuka, Jpn. J. Appl. Phys. **20** 1821-1832 (1981) .

15. B. Rodricks, C. Brizard, R. Clarke, W. Lowe, "Time-resolved x-ray scattering using spatially-dispersed optics and a CCD detector" to be submitted to Nuclear Instrum. and Meth.

16. R. Clarke, W. Passos, W. Lowe, B. Rodricks, C. Brizard, Physical Review Letters, Vol. **66**, N.3, 1991.

17. R. Clarke, W. Lowe, B. Rodricks, C. Brizard, "Time-resolved X-ray Scattering Studies," Proc. SPIE 1990 Int. Symposium on Optical and Optoelectronic Applied Science and Engineering, San Diego, 1990.

18. C. Brizard, B. Rodricks, "Programmable CCD imaging system," submitted to Optical Engineering.

TABLE I: Diffracted peaks observed at an energy of 7 keV (classified with increasing 2θ).*

	(hkl)	I/I_1	d(Å)	2θ
Fe_3B	321	100	2.088	50.20
	330,112	100	2.028	51.79
α-Fe	110	100	2.0268	51.83
Fe_2B	211	100	2.0129	52.21

*The data are taken from the joint comittee on powder diffraction standards (JCPDS) 1983. The column I/I_1 provides the relative intensities for one compound. The strongest line in the pattern has a ratio of 100. The parameter d(Å) is the interplanar spacing. Note that the Fe_3B (330,112) and α-Fe (110) reflections coincide.

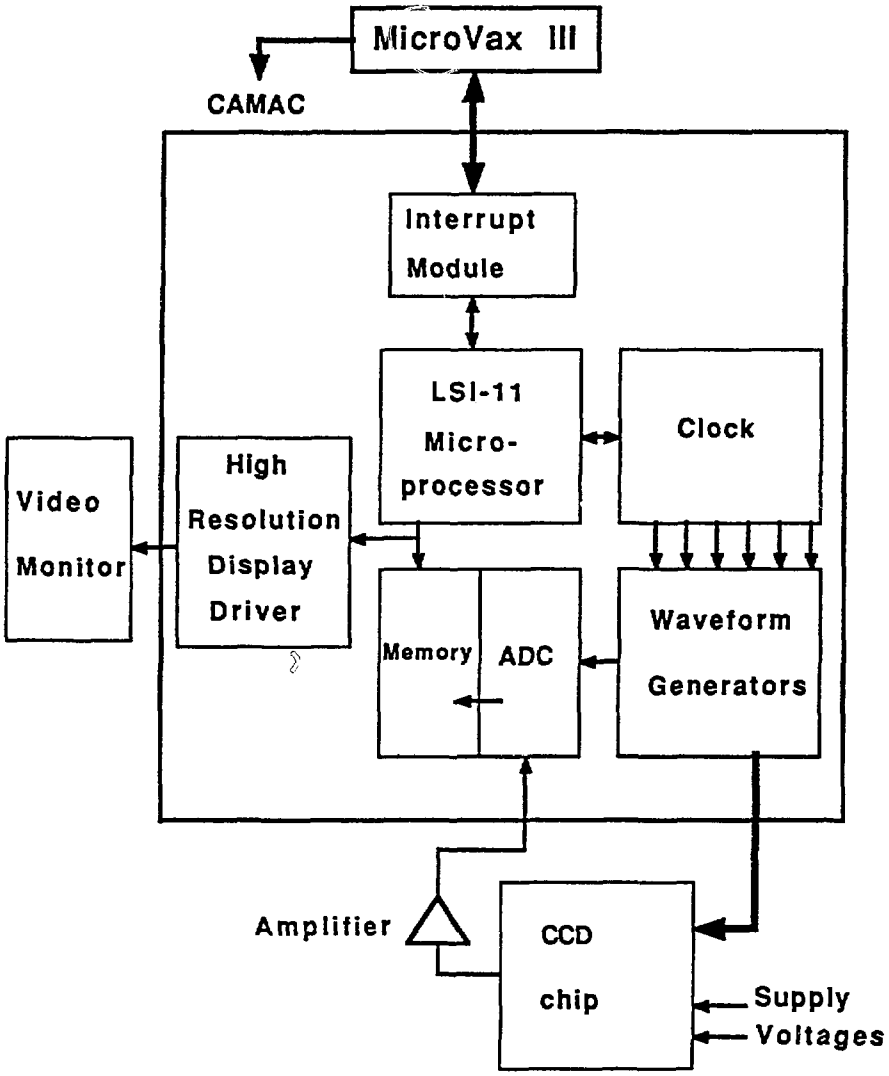

Fig. 1: General electronic architecture of the CCD detector. The system is controlled by a MicroVax III and the electronics are CAMAC-based.

Fig. 2a

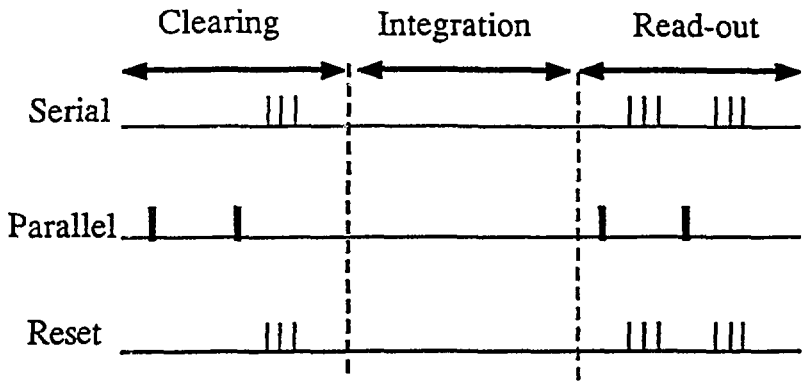

Fig. 2b

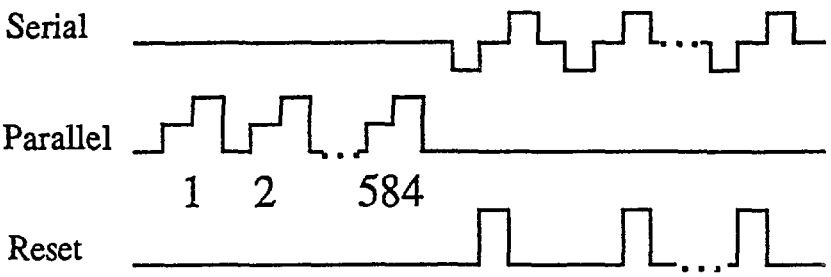

Fig. 2c

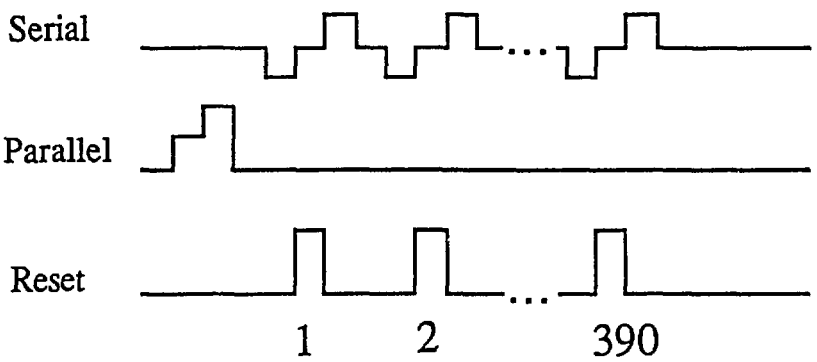

Fig. 2a: Timing diagram of the Texas Instruments TI 4849 virtual-phase CCD chip.
Fig. 2b: Clearing sequence for the TI 4849.
Fig. 2c: Read-out sequence for the TI 4849.

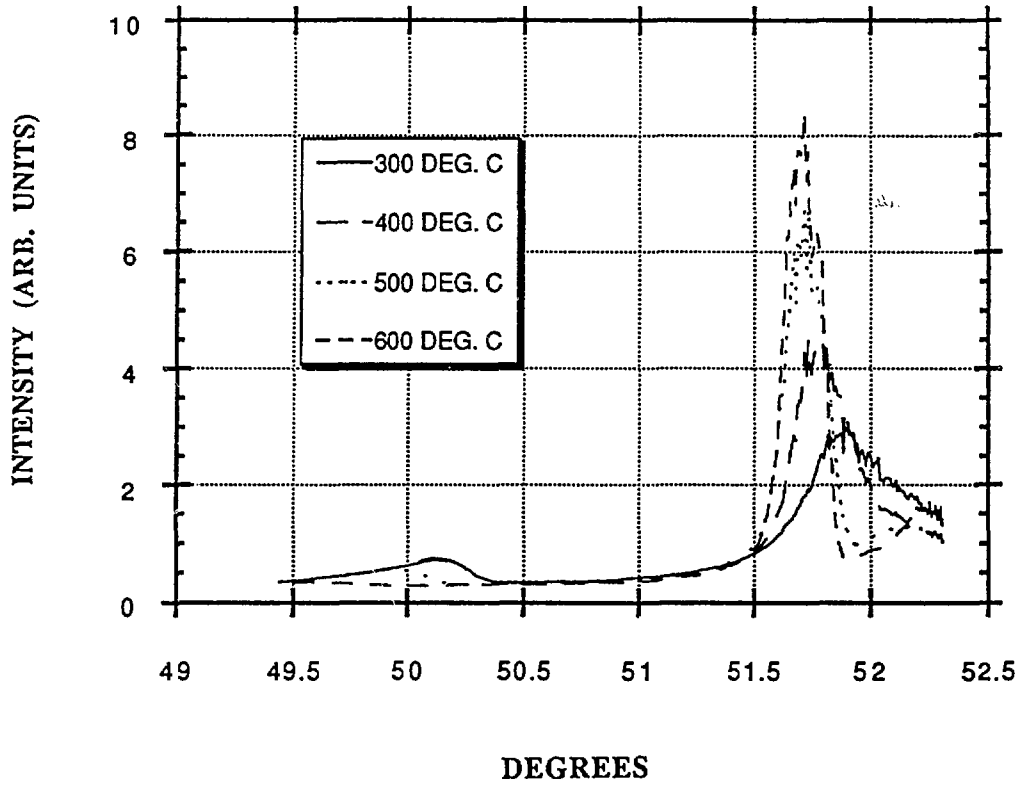

Fig. 3: Diffracted peaks obtained during the *in situ* crystallization of $Fe_{80}B_{20}$: Fe_3B, α-Fe, Fe_2B from low to high 2-theta angles. This set of data was taken at temperatures ranging from 300° C to 500° C.